Ph.D. 3rd year presentation

on

Power Stages and Control of Wireless Power Transfer Systems (WPTSs)

Presented by

Rupesh Kumar Jha

Tutor: Prof. Giuseppe Buja

Department of Industrial Engineering
University of Padova - Italy

Laboratory of
Electric System for Automation and Automotive (ESAaA)

PRESENTATION OUTLINE

1. Wireless Power Transfer
2. Resonant topologies
3. Figure of merits
4. Analysis and comparison of two WBC arrangements
5. Frequency mismatch analysis
6. High power WBC system
7. Dynamic modeling of WPTS
8. Conclusion
9. Personal training plan
10. References

1. WIRELESS POWER TRANSFER

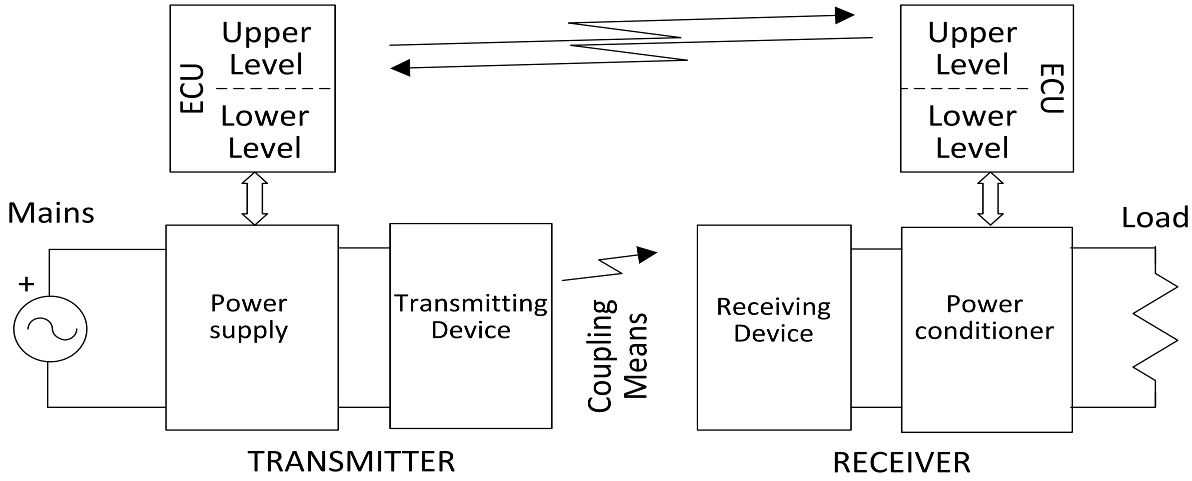

Magnetic WPT is used for EV charging

- **Electric WPT (Capacitive)**
  Suitable for low power transfer
- **Magnetic WPT (Inductive)**
  Suitable for comparatively large power transfer
- **Electromagnetic (radiation) WPT**
  More suitable for long distance (in the range of Km)

The three main components of a WPT system are

- Power supply of the transmitting coil
- Coupled coils
- Power conditioner for proper load supply

INDUCTIVE SCHEME

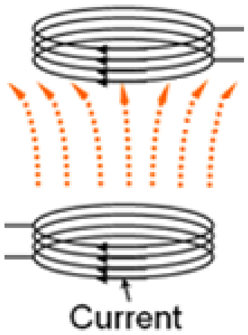

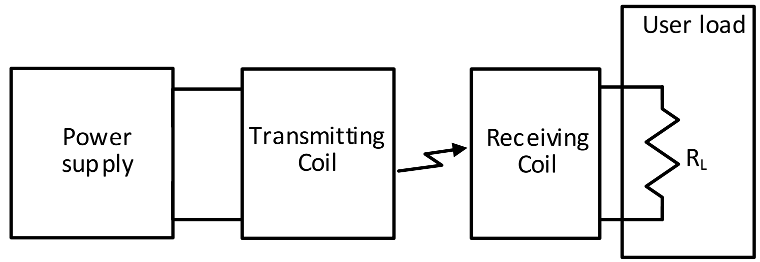

Inductive

- Drawback of Inductive power transfer

  i) Not efficient

  ii) Need large VA sizing of power source

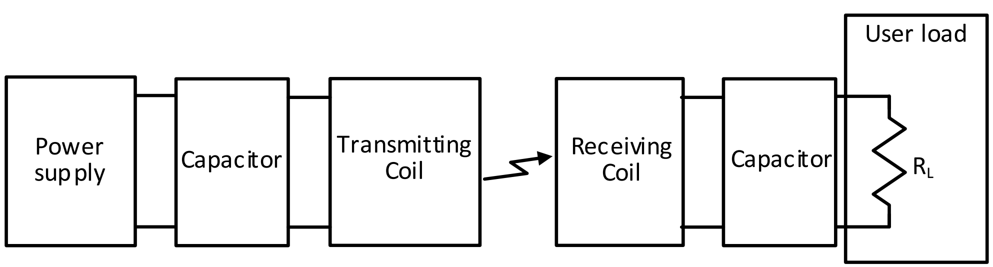

Resonant

2. RESONANT TOPOLOGIES

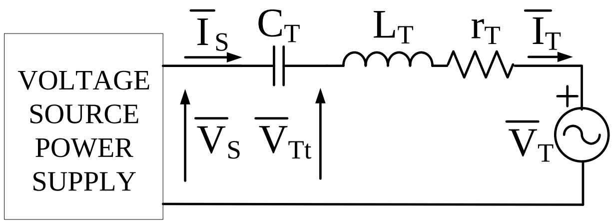

Transmitter scheme with series resonance

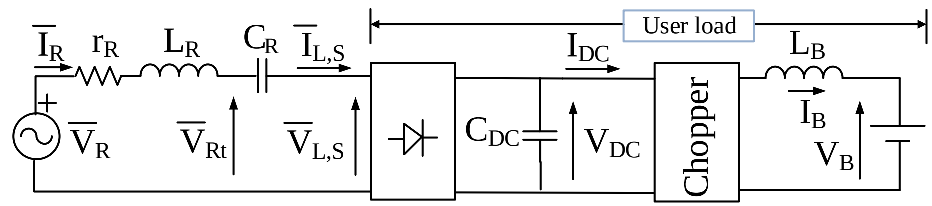

Receiver scheme with series resonance

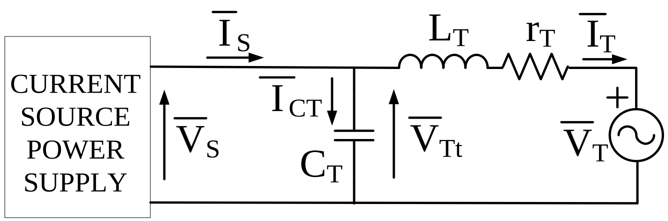

Transmitter scheme with parallel resonance

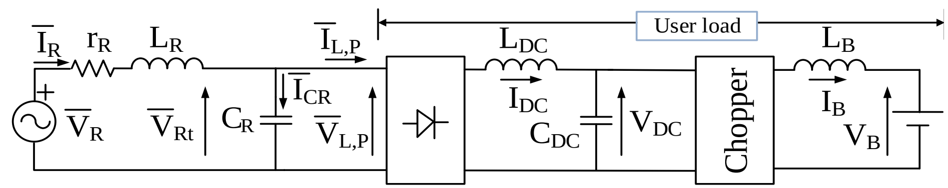

Receiver scheme with Parallel resonance

- According to the connection (in series or in parallel) of capacitors with the coils there are

  (1) Series-Series (SS) topology (3) Parallel-Series (PS) topology

  (2) Series-Parallel (SP) topology (4) Parallel-Parallel (PP) topology

PROTOTYPE FOR ELECTRIC CITY-CAR

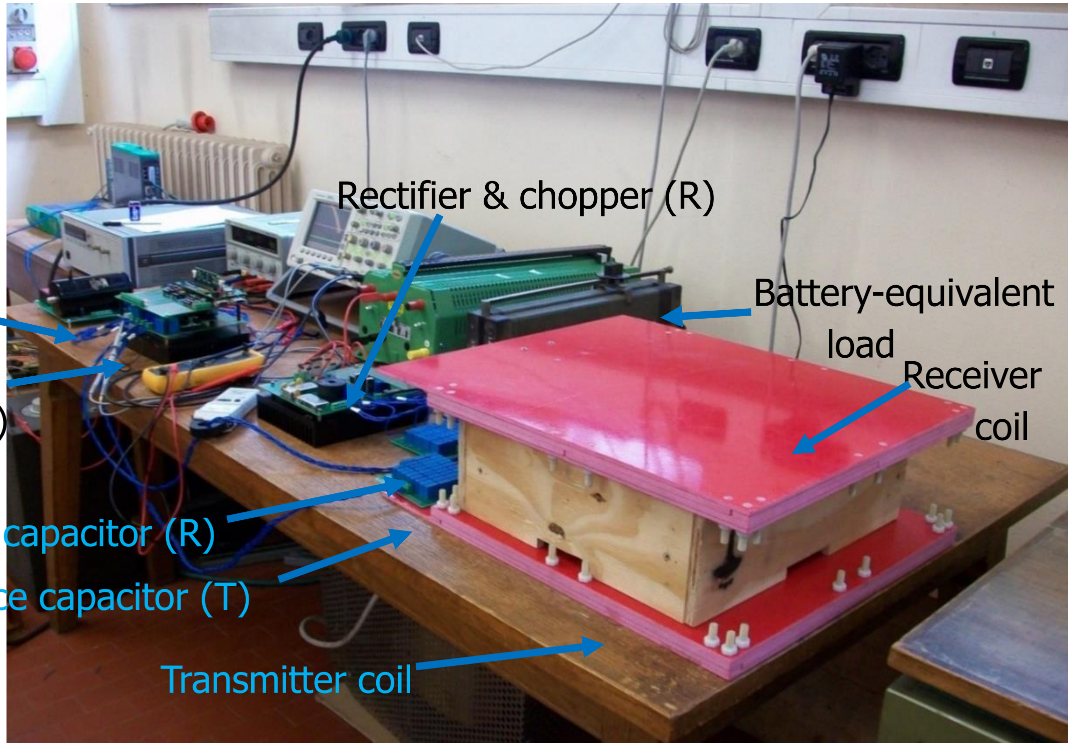

Electric city-car

Coil without protective cover

PROTOTYPE FOR ELECTRIC CITY-CAR Cont'd

BATTERY AND WBC SETUP CHARACTERISTICS

Data	Symbol	Value
DC bus voltages	V_{DC}	65 V
Nominal power	P_N	560 W
Trans. and rec. coils inductances	L_T, L_R	120 µH
Trans. and rec. coils parasitic resistances	r_T, r_R	0.5 Ω
Trans. and rec. resonant capacitances	$C_{T,}$ C_R	29 nF
Coil mutual inductance	M	30 µH
Coupling coefficient	k	0.25
Supply angular frequency	ω	2π·85000 rad/s

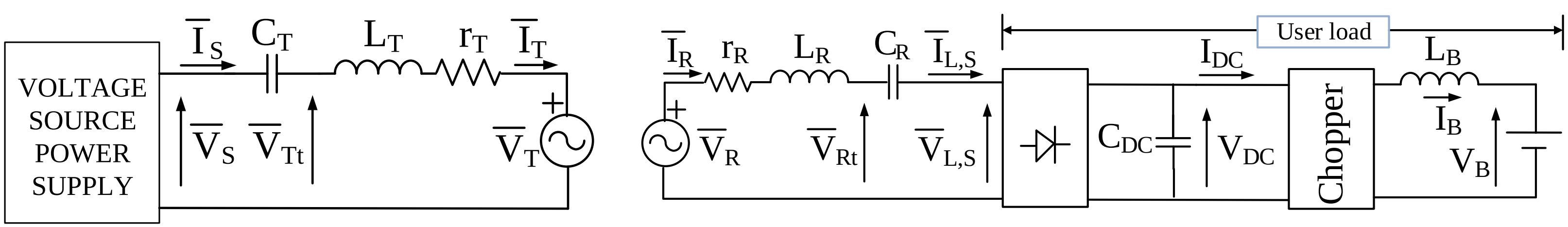

3. FIGURES OF MERIT

WBC performance is investigated in terms of **efficiency** η, power sizing factor of the supply inverter (**SIPSF**) and power sizing factor of the coil coupling set (**CCPSF**). They are defined as

$$\eta \triangleq \frac{P_B}{P_S}$$

$$SIPSF \triangleq \frac{A_I}{P_N}$$

$$CCPSF \triangleq \frac{A_T + A_R}{P_N}$$

P_B	Power absorbed by the battery
P_S	Active power delivered by the supply inverter
A_I	Power sizing of supply inverter
A_T	Power sizing of the transmitter coil
A_R	Power sizing of the receiver coil

$$A_I = max[V_S]max[I_S]$$

$$A_T = max[V_{Tt}]max[I_T]$$

$$A_R = max[V_{Rt}]max[I_R]$$

- **SIPSF** and **CCPSF** are indexes of both cost and volume of WBC with respect to the nominal charging power of the battery.

BATTERY CHARGING PROFILE

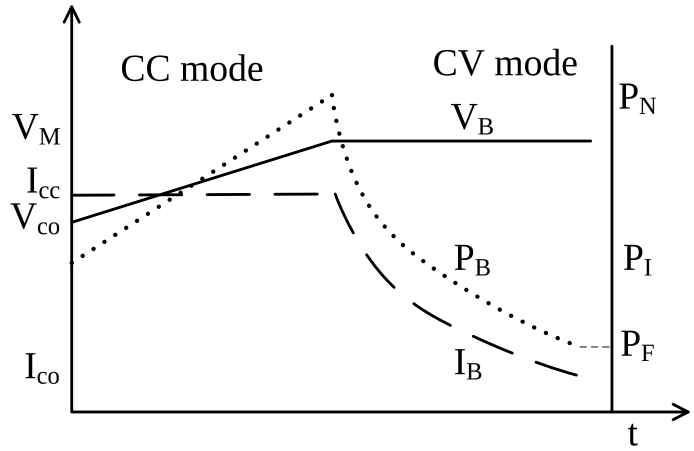

Battery charging profiles of voltage (**solid line**), current (**dashed line**), and power (**dotted line**).

Symbol	Data
I_B , V_B	Battery current and voltage
I_{CC} , I_{co}	I_B in CC mode and at cutoff
V_M ,V_{co}	V_B in CV mode and at cutoff
P_B	Power absorbed by battery
P_I , P_F	P_B at the beginning and completion of battery charging
P_N	Nominal battery power defined as $V_M I_{CC}$

EFFICIENCY COMPARISON

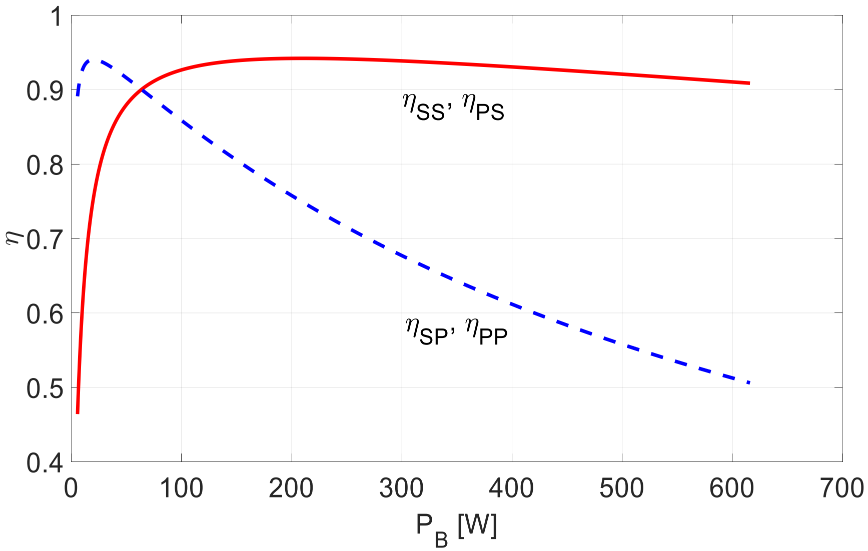

Blue dashed line for SP, PP and **red** solid line for SS, PS topology

- Efficiency of the SP and PP topologies exceed the SS and PS one only when P_B is lower than 0.08 P_N, which is below the minimum power of 0.1 P_N required to charge EV.
- Maximum efficiency is nearly the same for all the topologies and is of about 94%; the power in correspondence of the maximum efficiency is 0.28 P_N for the SS and PS topologies and 0.02 P_N for the SP and PP one.

FOMS CALCULATIONS

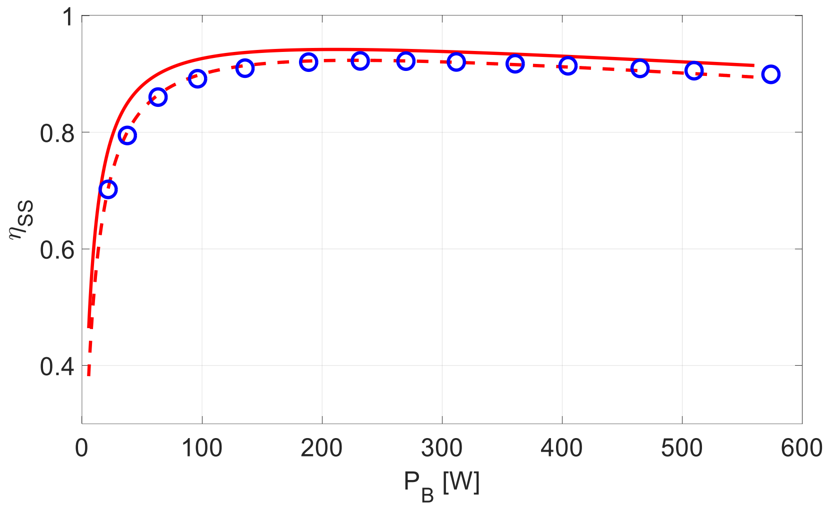

Efficiency by considering r_T and r_R equal to 0.5 Ω (in **red solid** line) and 0.6 Ω (in **red dotted** line) along with experimental result in **blue circles**

Topology performance						
	η_{max}	A_I [VA]	A_T [VA]	A_R [VA]	SIPSF	CCPSF
SS	0.94	560	1000	5895	1	12.3
SP	0.94	3896	55913	566	6.9	100.8
PS	0.94	676	1000	5895	1.2	12.3
PP	0.94	3645	55913	566	6.5	100.8

4. ANALYSIS AND COMPARISON OF TWO WBC ARRANGEMENTS

The two arrangements for a WBC receiver charge the battery either in a straight- forward manner through a diode rectifier or through a chopper in cascade to the diode rectifier, and controls the voltage of the power source in the transmitter to adjust the power absorbed by the battery.

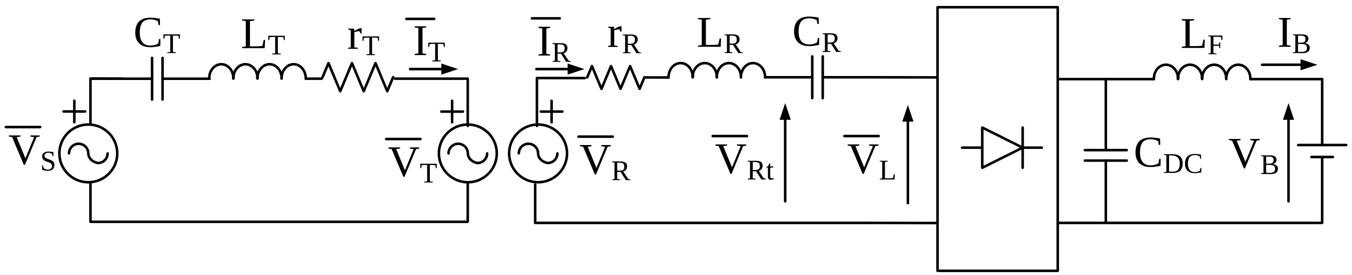

WBC arrangement without chopper i.e. (arrangement #1)

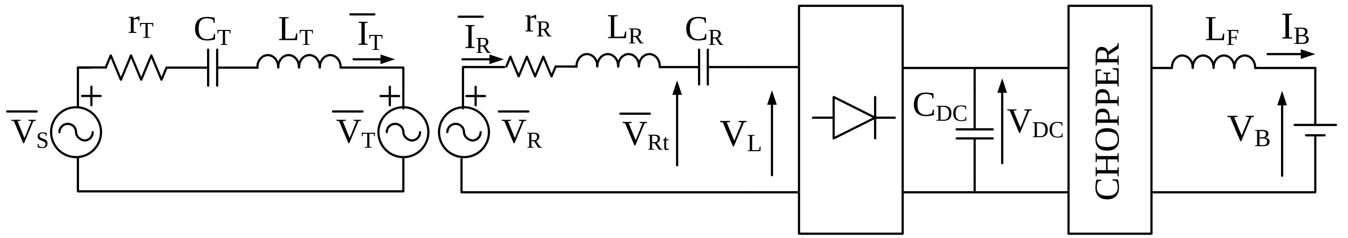

WBC arrangement with chopper i.e. (arrangement #2)

ARRANGEMENT COMPARISON

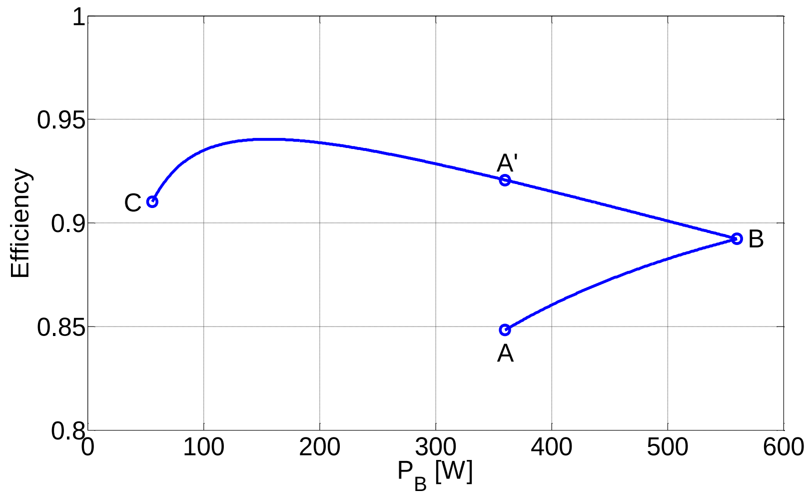

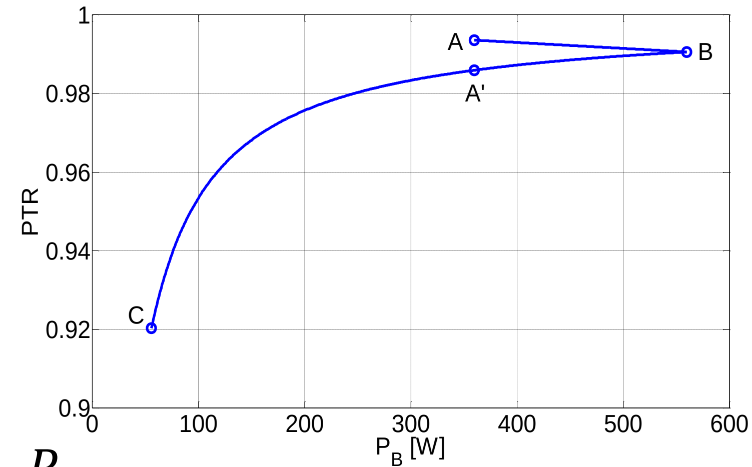

$$PTR \triangleq \frac{P_R}{P_S}$$

The curves of efficiency and PTR are ABC for arrangement #1 and A'BC for arrangement #2.

- **Arrangement #1**
  CC mode starts from point A and moves to B while CV mode starts from point B and continues till point C.

- **Arrangement #2**
  CC mode starts from point A' and moves to B while CV mode starts from point B and continues till point C.

V_{DC} EFFECT ON FOMS

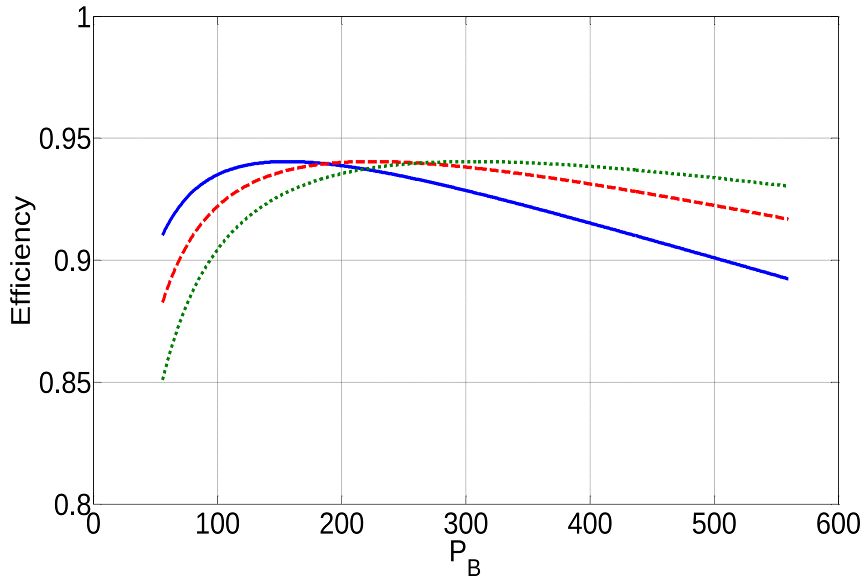

Efficiency for WBC arrangement #2 with V_{DC}=$\mathbf{V_M}$ (blue solid line), V_{DC}=**1.2** $\mathbf{V_M}$ (dashed red line) and V_{DC}=**1.4** $\mathbf{V_M}$ (green dotted line).

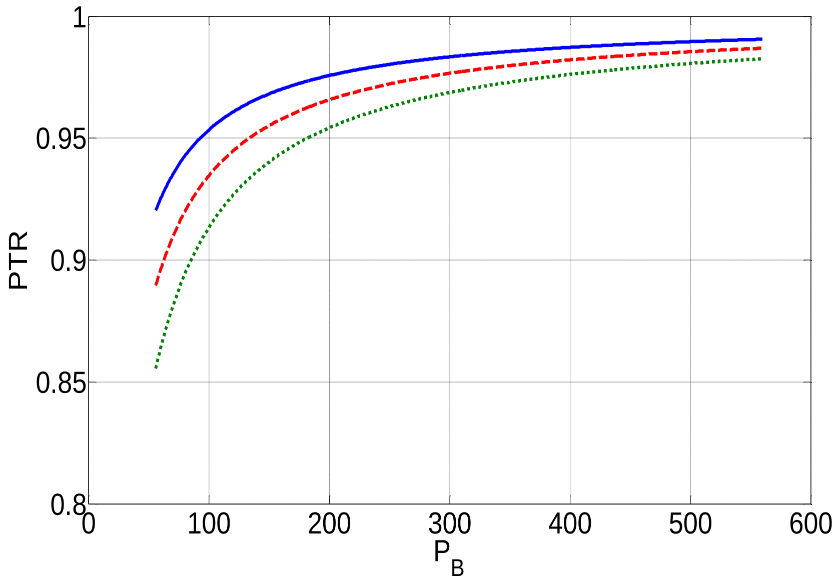

PTR for WBC arrangement #2 with V_{DC}=$\mathbf{V_M}$ (blue solid line), V_{DC}=**1.2** $\mathbf{V_M}$ (dashed red line) and V_{DC}=**1.4** $\mathbf{V_M}$ (green dotted line).

The SIPSF values calculated for the three values of V_{DC} by accounting for the parasitic resistances are: 1.12 for $V_{DC}=V_M$, 1.09 for $V_{DC}=1.2V_M$ and 1.07 for $V_{DC}=1.4V_M$, highlighting a small decrease of SIPSF at the higher values of V_{DC}

5. FREQUENCY MISMATCH ANALYSIS

- **Frequency mismatch**: resonance frequency of the transmitter and/or receiver differs from the supply frequency

Reason for frequency mismatch: deviation of the L, C components due to

- Thermal and ageing effects
- Construction/production tolerances
- Variation of coil distance (for cored coils)

Method of analysis

- Deviation of one parameter at the time
- Range of parameter deviation of ±10%
- Impact of the frequency mismatch determined on two figures of merit (FOMs): efficiency and SIPSF

Variable parameters	Efficiency (η) decreases *	SIPSF increases *
L_T , C_T	0%	1%
L_R , C_R	3%	35%

* at the extremities of the parameter deviation range

DIFFERENT TUNING SOLUTIONS

Three proposed solutions to have:

- transmitter stage resonance (**TSR**) by forcing voltage and current in the transmitter to be in phase in uncoupled conditions

$$\bar{V}_S = \boldsymbol{r}_T \bar{I}_T \quad \longrightarrow \quad \omega = \frac{1}{\sqrt{L_T C_T}}$$

- receiver stage resonance (**RSR**) by forcing current in the transmitter to be out of phase from current in the receiver

$$\bar{I}_T = j\left(\frac{R_L + \boldsymbol{r}_{\boldsymbol{R}}}{\omega M}\right)\bar{I}_R \quad \longrightarrow \quad \omega = \frac{1}{\sqrt{L_R C_R}}$$

- Input impedance resonance (**IIR**) by forcing voltage and current in the transmitter to be in phase in coupled conditions

$$\bar{V}_S = \bar{I}_T\left\{\boldsymbol{r}_T + \frac{(\omega M)^2}{R_L + \boldsymbol{r}_{\boldsymbol{R}}}\right\}$$

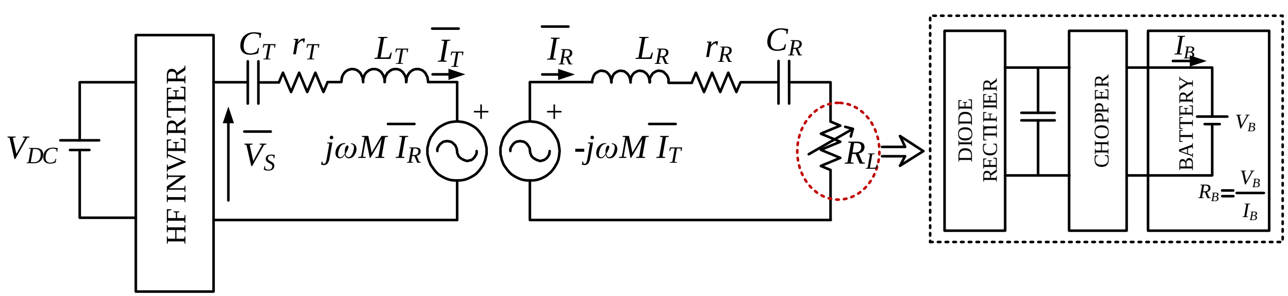

DIFFERENT TUNING SOLUTIONS Cont'd

Tuning solution	Variable parameters	Efficiency (η) decreases *	SIPSF increases *	Supply frequency
TSR	L_T , C_T	3%	33%	n.a.
RSR	L_R , C_R	1%	negligible	within SAE limit
IIR	L_T , C_T	2%	negligible	beyond SAE limit
	L_R , C_R	1%	negligible	

SAE, in its guideline TIR J2954, fixed the supply frequency of wireless battery chargers (WBC) in the range of 81.39-90 kHz

TUNING IMPLEMENTATION

- Implementation of RSR is not practical because it requires wireless transmission of high frequency receiver current. Then **IIR** is implemented.

- Simulation is carried out by MATLAB/Simulink by assuming a deviation of L_R of -10%

  - Tuning scheme is able to reset the phase shift during the first 40 ms of operation.

  - Supply frequency increases of about 0.35% at steady state

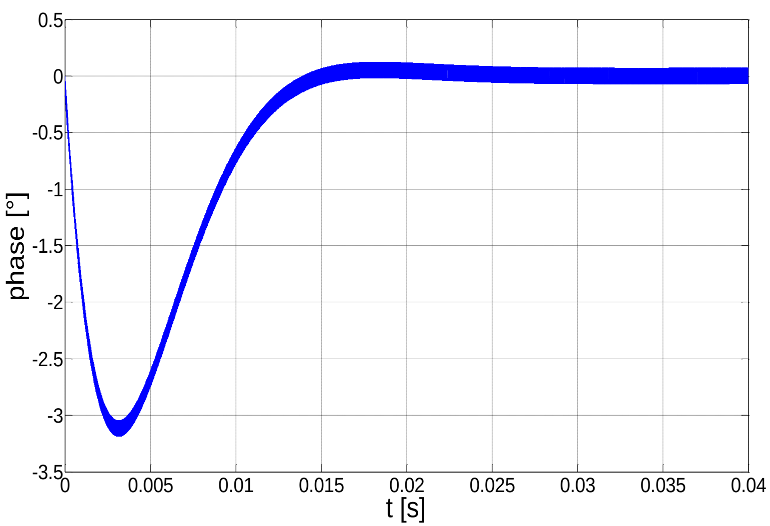

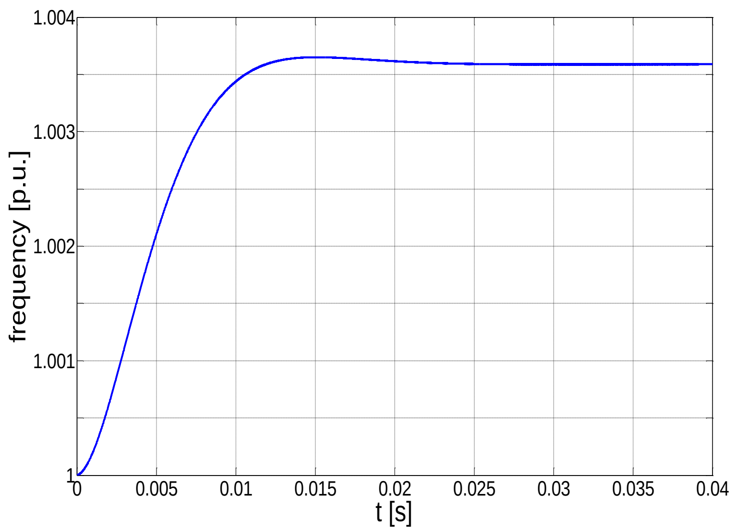

6. HIGH POWER WBC SYSTEM

- **Need for High power WBC system**
- Fast charging
- Increases the running time of EVs in one charge
- Makes adaptable the electric bus and the train

- **Topic covered**
- Core materials
- Power supply architecture
- Coil geometry

- **Power supply architecture**
- Single stage (using matrix converter)
- Two stage
- Parallel

- **Magnetic core material**

Magnetic material (60μ)	Change in μ_i [%]*	Magnetizing force [Oe] **	Relative cost ***	Core loss (mW/cm^3) ****	Shape	B_{sat} (T)
MPP	96	32	10-18	12.6	T	0.88
High flux	90	47	7-9	27.8	T	1.48
Sendust	98	30	2-3	12.9	T, E & B	0.89
Fluxsan	97	40	2-4	24.2	T, E & B	1.67
Optilloy	96	41	6-7	15.9	T	1.3

Here
T stands for toroidal shape
B stands for block shape

* Upto 1MHz

** DC magnetization force to reach 90% of initial permeability

*** w.r.t. iron powdered core for 25 mm toroidal shape by Micrometals

****At 100 kHz

COIL GEOMETRY

Why DD coil

- Single-sided flux paths
- Average flux path height that is proportional to half of the length of the coil
- Insensitivity to aluminum shielding
- Low leakage flux

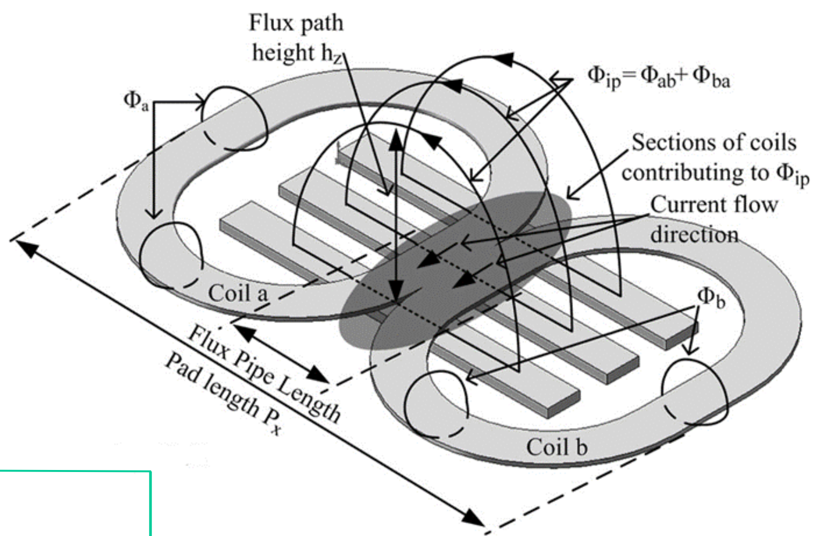

Simplified model of a DD coil

Coil design

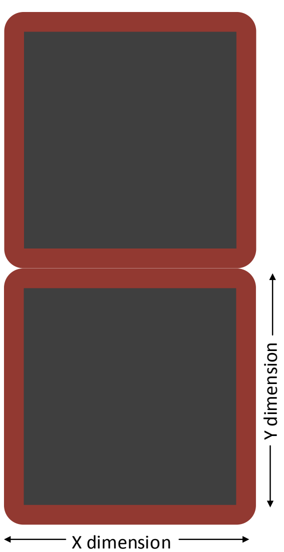

Parameters	Value (in mm)
Core thickness	10
Core X dimension	375
Core Y dimension	435
Coil X dimension	375
Coil Y dimension	450
Coil distance	190
Wire radius	4.5
Turn No	4

COIL GEOMETRY Cont'd

- **Case of study**
  - A track of three transmitting coil (DD)
  - One receiving coil (DD)
  - Receiver or EV moves along the track coil centers
  - EV speed is constant
  - All coils are identical

JMAG as Simulation tool

- It works on finite element method
- Gives accurate solutions for boundary value problems

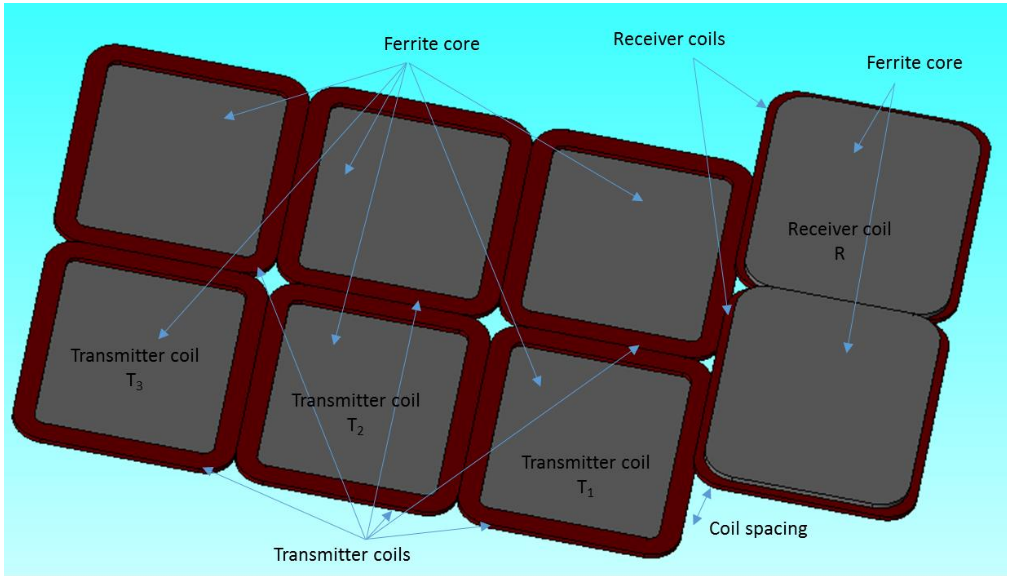

Simulation model created using JMAG

COIL GEOMETRY Cont'd

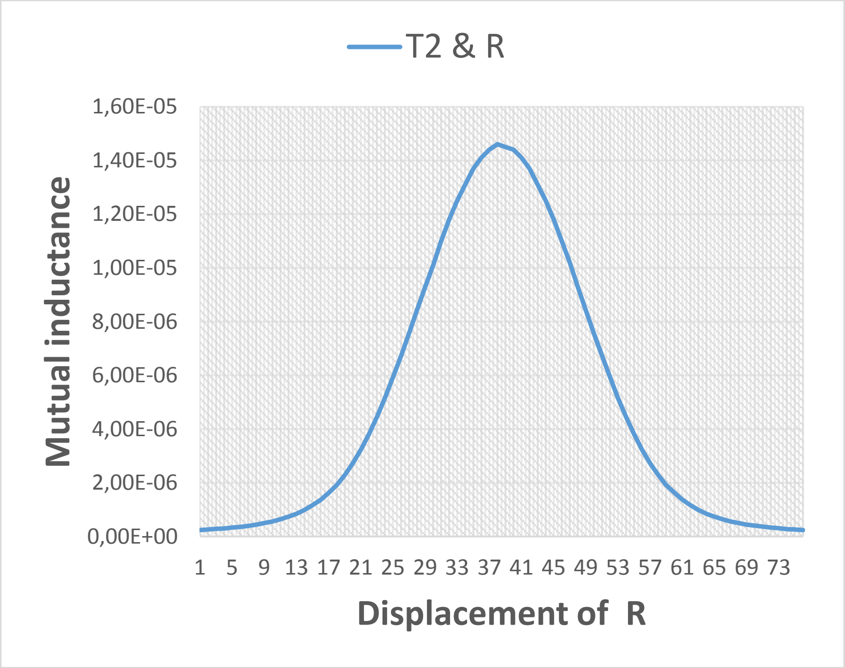

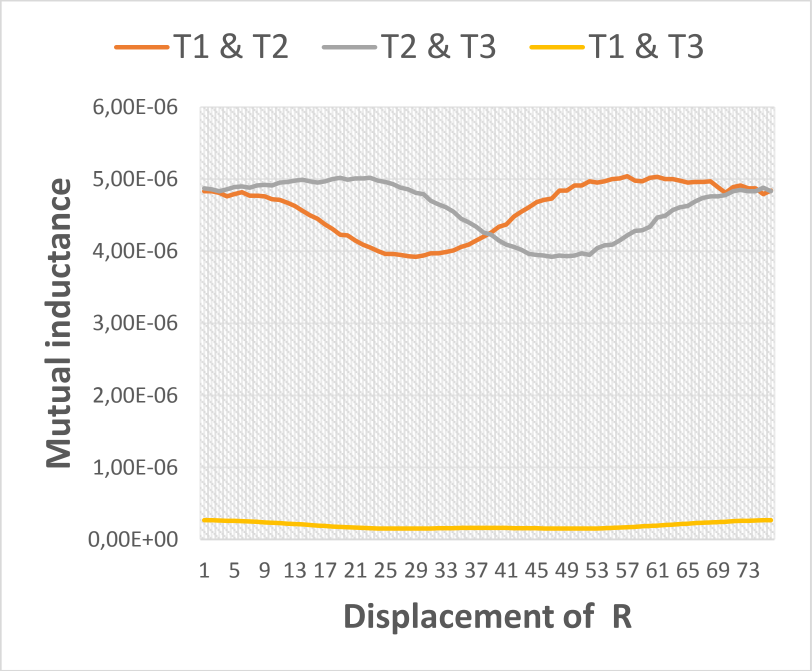

Mutual inductance between T_2 and R when R is moving.

Mutual inductance among all the transmitter coil when R is moving

7. DYNAMIC MODEL OF WPTSs WITH GSSA METHOD

➢ The dynamic model of a WPTS that considers the envelope of the alternating signal. Generalized state space averaging (GSSA) and Laplace phasor transform (LPT) technique are generally used for this.

GSSA method

➢ **GSSA** method is based on the fact that any waveform can be approximated in the form of Fourier series representation for any finite interval using its first coefficient for state space mode.

$$x(\tau) = \sum_{k=-\infty}^{k=+\infty} \langle x \rangle_k(t)\, e^{jk\omega_s\tau}, \quad \tau \in [t - T_s, t]$$

$$\langle x \rangle_k(t) = \frac{1}{T_s} \int_{t-T_s}^{t} x(\tau)\, e^{-jk\omega_s\tau}\, d\tau$$

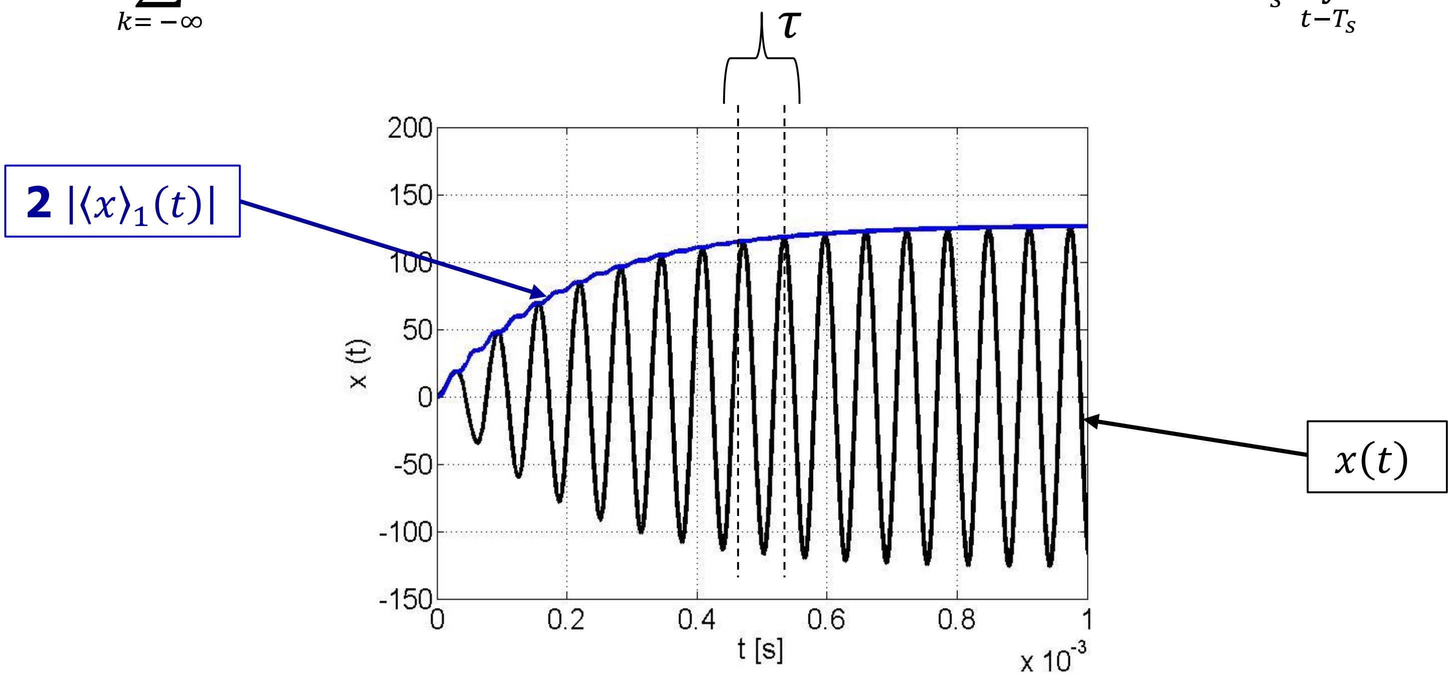

DYNAMIC MODEL OF SYSTEM WITH LPT METHOD

- Laplace phasor transform (LPT) technique basically converts rotatory ac domain circuit into stationary domain circuit

$$x(t) = Re\{\,\bar{x}(t)e^{j\omega t}\}$$

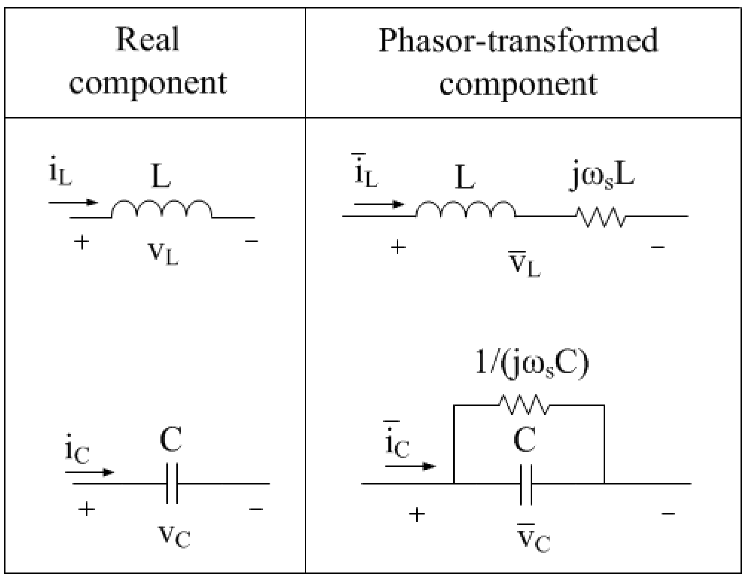

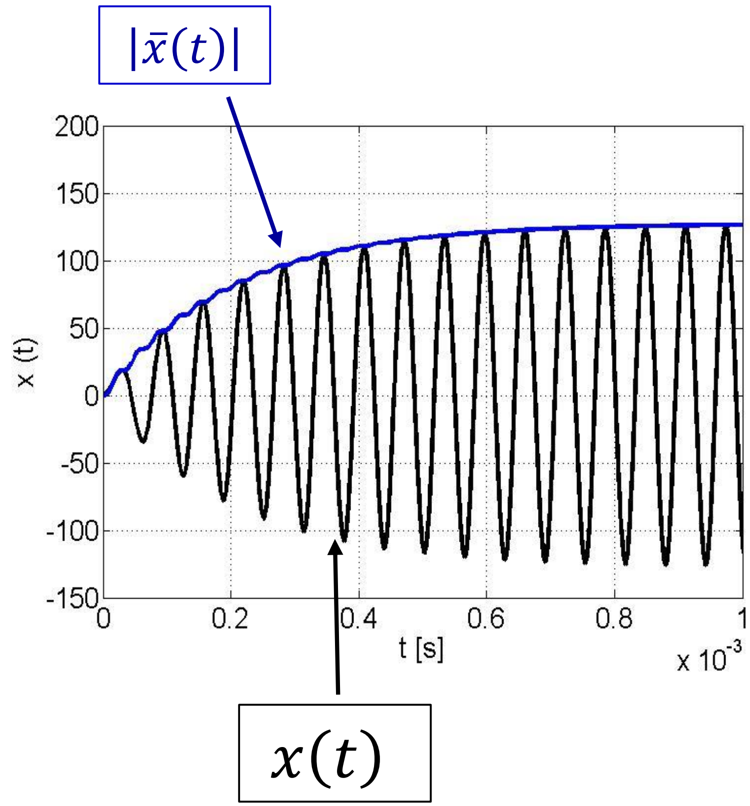

STEP RESPONSE

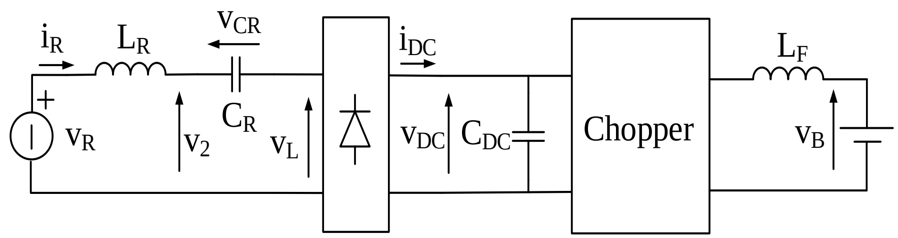

Receiving circuit of a resonant WPT EV charger,

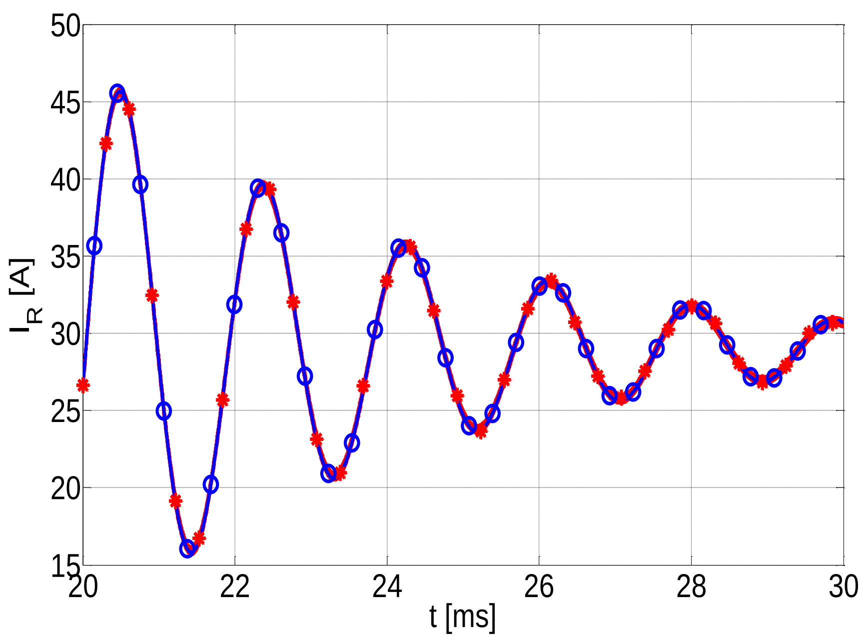

Envelopes of the step responses obtained by simulation (**red stars**) and by GSSA and LPT (**blue circles**).

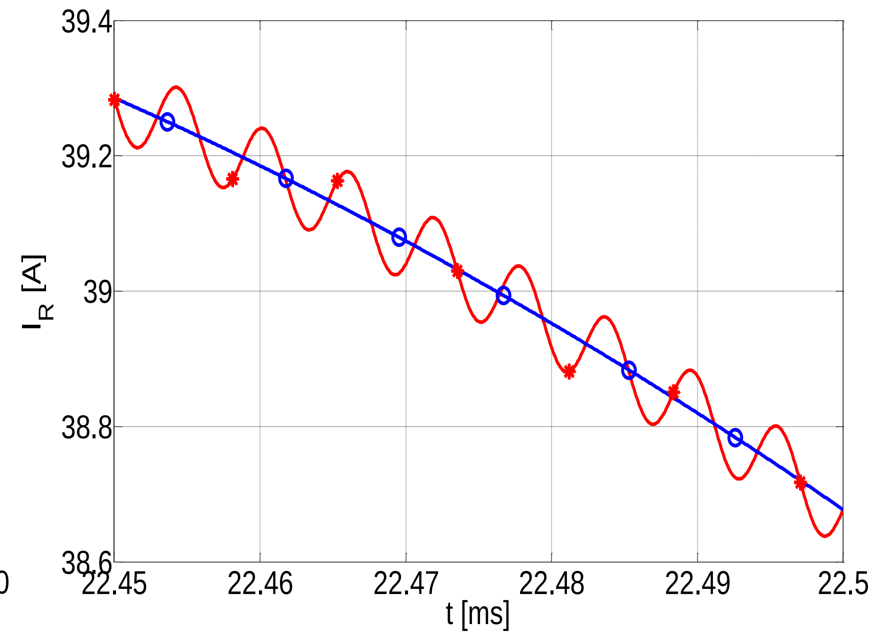

Magnification of a time interval of the envelopes (**red** stars refer to the **LPT** method, **blue** circles to **GSSA** method and simulation).

8. CONCLUSIONS

- Comparative study of different resonant topologies is done where SS outperforms on all.
- Favorable SS topology with two WBC arrangements have been examined, where receiver using chopper is found to be more suitable for WBC system.
- Three frequency updates technique such as TSR, RSR and IIR are studied and analyzed for variation of reactive elements from their nominal values. IIR is concluded to be the most feasible technique.
- Continuing with high power WBC system, i) three architectures of power supply is studied, ii) sendust and DD coil are found to be suitable core material and coil geometry respectively.
- For control purpose, modeling of system is done with two methods such as GSSA and LPT.

9. PERSONAL TRAINING PLAN

EDUCATIONAL ACTIVITIES ACTIVATED BY THE STMS PHD COURSE							
Course/Seminar (Period/Date)	Teacher	Duration (hours) of course / seminar	Attainable ECTS credits	Frequency (YES/NO)	Exam (YES/NO and type)*	Date of exam**	Attained ECTS credits
Fundamentals of measurements and PC-based applications	Prof. Debei, Prof. Lancini	20	4	SI	SI (Report)		4
Space systems and their control	Prof. Francesconi, Prof. Lorenzini	20	4	SI	Written Exam	September 2015	4
Presentation of Research Proposal	Prof. G. Naletto	10	2	SI	SI (Write-up proposal)		2
Space optics and detectors	Prof. Naletto, Prof.ssa Pelizzo	20	4	SI	Written Exam	June 2015	4
Admission to Ph.D. presentation			1/3	SI	Presentation	November 2014	1/3
Attendance to admission presentation of new Ph.D. students			1/6	SI	Attendance only	October 2015	1/6
Attendance to admission presentation of new Ph.D. students			1/6	SI	Attendance only	October 2016	1/6
Attendance to admission presentation of new Ph.D. students			1/6	SI	Attendance only	October 2017	
Presentation after 1st year			1/2	SI	Presentation	October 2015	1/2
Presentation after 2nd year			1/2	SI	Presentation	October 2016	1/2
Presentation after 3rd year			1/2	SI	Presentation	October 2017	
15*2 hours long Specialistic Seminars offered by the Ph.D. School/Course (0.4 ECTS each with final discussion)	Various Professors	30	6	SI	Attendance + discussion/ presentation	From March 2015 to end of Ph.D.	4
OTHER EDUCATIONAL ACTIVITIES							
Title of the activity (Date/Period)	Teacher	Duration (hours) of activity	Attainable ECTS credits	Frequency (YES/NO)	Exam (YES/NO and type)*	Date of exam**	Attained ECTS credits
Electric Road Vehicles	Prof. G. Buja	48	6.0	SI	SI (Exam)		6
External seminars, congresses, didactics support activities		32	1.67	SI	Attendance only		1.28
Summer Course on Power Electronics and Applications	Various Prof.	80	3	SI	Attendance and discussion		3
Total of ECTS credits attainable in educational activities (>30):			30	Total of ECTS credits attained in educational activities: date 05 10 2017			30

10. REFERENCES

- Ji. Kim, Jon. Kim, S. Kong, H. Kim, I. Suh, N. Suh, D. Cho, Jou. Kim, and S. Ahn, "Coil Design and Shielding Methods for a Magnetic Resonant Wireless Power Transfer System," *Proceedings of the IEEE*, vol. 101, no. 6, pp.1332-1342, 2013.
- V.J. Brusamarello, Y.B. Blauth, R. Azambuja, and I. Muller, "A study on inductive power transfer with wireless tuning," Proc. of IEEE Int. Instrumentation and Measurement Technology Conf. (I2MTC), 2012, pp. 1098–1103.
- C. Fernandez, O. Garcia, R. Prieto, J. Cobos, S. Gabriels, and G.Van Der Borght, "Design issues of a core-less transformer for a contact-less application," Proc. of. IEEE 17th Applied Power Electronics Conference and Exposition, 2002, pp. 339-345.
- Y. Kaneko and S. Abe, "Technology trends of wireless power transfer systems for electric vehicle and plug-in hybrid electric vehicle," Proc. IEEE 10th Int. Conf. on Power Electronics and Drive Systems (PEDS), 2013, pp. 1009–1014.
- H. Takanashi, Y. Sato, Y. Kaneko, S. Abe, and T. Yasuda, "A large air gap 3 kW wireless power transfer system for electric vehicles," Proc. IEEE Energy Conversion Congr.&Exposit., 2012, pp. 269–274.
- C.-J. Chen, T.-H. Chu, C.-L. Lin, and Z.-C. Jou, "A Study of Loosely Coupled Coils for Wireless Power Transfer," IEEE Transactions on Circuits and Systems - IT: Express Briefs, Vol. 57, N. 7, pp. 536-540, 2010.
- R.R. Harrison, "Designing efficient inductive power links for implantable devices," Proc. of IEEE Int. Symposium on Circuits and Systems (ISCAS), 2007, pp. 2080–2083.
- M. Bertoluzzo, M.K. Naik, and G. Buja, "Preliminary investigation on contactless energy transfer for electric vehicle battery recharging," Proc. of IEEE Int. Conf. on Industrial and Information Systems (ICIIS), 2012, pp. 1-6.
- S. Chopra and P. Bauer, "Analysis and design considerations for a contactless power transfer system," Proc. IEEE Telecommunications Energy Conf. (INTELEC), 2011, pp. 1–6.
- C. Wang, G.A. Covic, and O.H. Stielau, "Power transfer capability and bifurcation phenomena of loosely coupled inductive power transfer systems," IEEE Trans. Ind. Electron., vol. 51, no. 1, pp. 148–157, Feb. 2004.
- C. Wang, O.H. Stielau, and G.A. Covic, "Design considerations for a contactless electric vehicle battery charger," IEEE Trans. Ind. Electron., vol. 52, no. 5, pp. 1308–1314, Oct. 2005.
- K.N. Mude, M. Bertoluzzo and G. Buja, "Design of contactless battery charger for electrical vehicle," Proc. of IEEE Int. Africa Conf. (AFRICON), 2013, pp.1091-1096.

11. PUBLICATIONS

- R.K. Jha, S. Giacomuzzi, G. Buja, M. Bertoluzzo, and M.K. Naik, “Efficiency and sizing power of SS vs. SP topology for wireless battery charging,” in proc. of IEEE International Conference on Power Electronics and Motion Control (PEMC), 2016, Varna, Bulgaria.

- G. Buja, R.K. Jha, M. Bertoluzzo, and M.K. Naik, “Analysis and Comparison of Two Wireless Battery Charger Arrangement for Electric Vehicles,” *Chinese Journal of Electrical Engineering*, vol. 1, no. 1, Dec. 2015.

- M. Bertoluzzo, R.K. Jha, and G. Buja, “Series-series resonant IPT system analysis under frequency mismatch,” in proc. of IEEE Industrial Electronics Society (IECON), 2015, pp. 439-444.

Thank you for your kind attention